

Short Note

N,N'-Dibutyloxamide

 Enrico Podda ^{1,2} , Eleanor Dodd ³, Massimiliano Arca ¹ , M. Carla Aragoni ¹ , Vito Lippolis ¹ , Simon J. Coles ³ and Anna Pintus ^{1,*} 
¹ Department of Chemical and Geological Sciences, University of Cagliari, Cittadella Universitaria, S.S. 554 bivio Sestu, 09042 Monserrato, CA, Italy

² Centre for Research University Services (CeSAR), University of Cagliari, Cittadella Universitaria, S.S. 554 bivio Sestu, 09042 Monserrato, CA, Italy

³ UK National Crystallography Service, School of Chemistry, Faculty of Engineering and Physical Sciences, University of Southampton, Southampton SO17 1BJ, UK

* Correspondence: apintus@unica.it

Abstract: *N,N'*-dibutyloxamide (**1**) was prepared by reacting diethyloxalate with *n*-butylamine in ethyl alcohol and characterized by microanalytical techniques, FT-IR, and NMR spectroscopy. Crystals suitable for single crystal X-ray diffraction (SC-XRD) were obtained from an acetonitrile solution of **1**, and the structural characterization showed the presence of intermolecular hydrogen bonding interactions.

Keywords: *N,N'*-dialkylloxamides; oxalamides; oxamide ligands; oxalic acid derivatives; XRD

1. Introduction

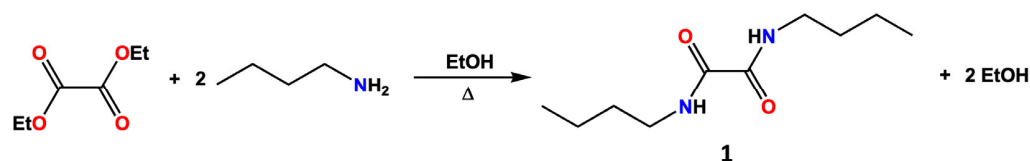
Oxamic acid derivatives are an important class of compounds with applications in fields as varied as medicine [1,2], organic synthesis [3,4], and cultural heritage [5–8]. In particular, the oxamide fragment can be found in various compounds of synthetic relevance, including biologically active compounds [9,10], precursors of widely used agents such as ethylene glycol [11,12], and ligands [13,14].

In this context, *N,N'*-dibutyloxamide (**1**) was employed in recent years as a bridging ligand in polynuclear rhenium, ruthenium, and manganese complexes [15–19], several of which have been structurally characterized. Despite this, the crystal structure of *N,N'*-dibutyloxamide has not been reported to date.

Herein, we report on the spectroscopic and structural characterization of *N,N'*-dibutyloxamide (**1**), which was synthesized from diethyloxalate and *n*-butylamine.

2. Results and Discussion

N,N'-disubstituted oxalamides can be prepared through the reaction of oxalyl chloride with the desired amine [20,21], and in more recent years, *N,N*-dibutyloxamide (**1**) and other derivatives were also synthesized by other methods, such as the catalytic carbonylation of amines [22,23]. In the present work, however, compound **1** was prepared through a modification of the classical synthetic route developed by Rice and co-workers in the 1950s [24] by reacting diethyloxalate with *n*-butylamine in ethanol (Scheme 1).



Scheme 1. Synthetic pathway for the preparation of compound **1**.

Compound **1** was fully characterized by means of elemental analysis, melting point determination, FT-IR, ¹H-, and ¹³C-NMR spectroscopy.



Citation: Podda, E.; Dodd, E.; Arca, M.; Aragoni, M.C.; Lippolis, V.; Coles, S.J.; Pintus, A. *N,N'*-Dibutyloxamide. *Molbank* **2023**, *2023*, M1677. <https://doi.org/10.3390/M1677>

Academic Editor: Rodrigo Abonia

Received: 31 May 2023

Revised: 23 June 2023

Accepted: 27 June 2023

Published: 29 June 2023



Copyright: © 2023 by the authors. Licensee MDPI, Basel, Switzerland. This article is an open access article distributed under the terms and conditions of the Creative Commons Attribution (CC BY) license (<https://creativecommons.org/licenses/by/4.0/>).

The middle infrared spectrum shows the characteristic peaks for the N–H stretching mode at 3298 cm^{-1} , in agreement with previous reports [22,23,25], while a series of peaks between 2850 and 3000 cm^{-1} can be assigned to the C–H stretching modes of the butyl chain, and those of the carbonyl groups fall at 1659 cm^{-1} (Figure S1).

The $^1\text{H-NMR}$ spectrum in CDCl_3 (Figure S2) shows the NH signal as a broad singlet falling at 7.46 ppm and the quadruplet signal of the $-\text{CH}_2-$ groups bound to the nitrogen atoms at 3.31 ppm , while those of the remaining protons of the *n*-butyl chain fall between 0.9 and 1.6 ppm . The $^{13}\text{C}\{^1\text{H}\}$ spectrum in the same solvent features a signal at 160 ppm assigned to the carbonyl moieties, while the remaining four signals resonating between 13 and 40 ppm can be attributed to the alkyl carbon atoms (Figure S3).

The recrystallization of compound **1** from acetonitrile yielded colorless block-shaped crystals that were structurally characterized by SC-XRD analysis.

Compound **1** crystallizes in the triclinic space group *P*-1 (Tables S1–S4), with half a molecule in the asymmetric unit (Figure 1). The two carbonyl groups are in the typical antiperiplanar conformation, with an $\text{O}=\text{C}-\text{C}=\text{O}$ torsion angle of 180° (Table S4), the oxalamide core being perfectly planar. The C–C, C=O, and C–N bond lengths (1.542 , 1.238 , and 1.327 \AA , respectively; Table S2) are very close to the corresponding average values of 1.533 , 1.226 , and 1.328 \AA , respectively, found for the 258 differently substituted free oxalamides retrieved from the Cambridge Crystallographic Data Centre (CCDC) [26]. The two *n*-butyl groups lie on opposite sides of the oxalamide core and are oriented perpendicularly to it in an extended conformation (C1–C2–C3–C4 dihedral angle: 179° ; Figure 1, Table S4). This is in analogy with the conformation adopted by compound **1** in metal complex $[\{(\text{CO})_3\text{Re}(\mu-\eta^4-1)\text{Re}(\text{CO})_3\}_2(\mu\text{-pbin})_2]$ (pbin = phenyl-1,4-bisisonicotinate) [16]. In contrast, in $[\text{I}(\text{CO})_3\text{Ru}(\mu-\eta^4-1)\text{Ru}(\text{CO})_3\text{I}]$, the *n*-butyl groups of **1** assume a folded conformation (dihedral angle within the alkyl chain: 67°) [18], and in the remaining complexes $[(\text{CO})_3\text{M}(\mu-\eta^4-1)(\mu\text{-bpp})\text{M}(\text{CO})_3]$ [$\text{M} = \text{Mn}, \text{Ru}$; bpp = bis-(4-pyridyl)propane] [17], $[\text{L}(\text{CO})_3\text{Mn}(\mu-\eta^4-1)\text{Mn}(\text{CO})_3\text{L}]$ ($\text{L} = 4\text{-picoline}, 4\text{-phenylpyridine}$), and $[\{(\text{CO})_3\text{Mn}(\mu-\eta^4-1)\text{Mn}(\text{CO})_3\}_2(\mu\text{-pby})_2]$ (pby = 4,4'-bipyridine) [19], the *n*-butyl chains are on the same side of the oxalamide core. The conformational variability in the abovementioned complexes can be ascribed to templating effects exerted by the metal ion, steric hindrance induced by other ligands, and other packing effects.

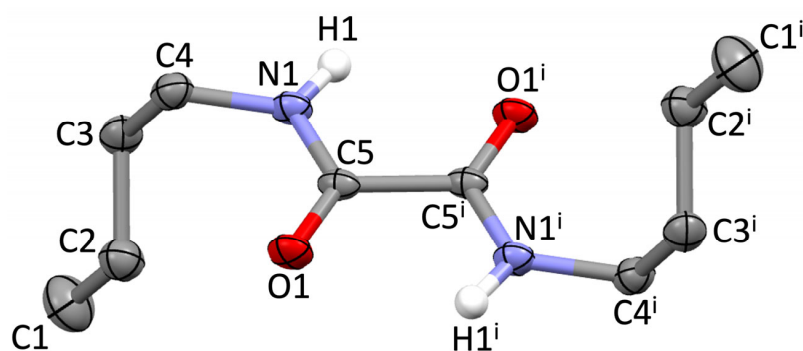


Figure 1. Molecular structure of **1** with the numbering scheme adopted. Displacement ellipsoids were drawn at the 50% probability level; hydrogen atoms were omitted for clarity, except for those of the N–H groups; $i = 1-x, 1-y, 1-z$.

In the crystal packing of compound **1**, N–H \cdots O hydrogen bonding interactions generating $R_2^2(10)$ motifs [27,28] can be observed between adjacent molecules whose oxalamide cores are coplanar (Figure 2a and Figure S4, Table 1), forming ribbons running along the *b*-axis. These interactions are similar to those observed for other oxalamides featuring alkyl [25,29,30] or aryl [31–33] substituents. The ribbons formed through the N–H \cdots O hydrogen bonds are held together by C–H \cdots O interactions between the carbonyl oxygens and the hydrogen atoms of the $-\text{CH}_2-$ groups bound to the nitrogen atoms (Figure 2b and Figure S4, Table 1); they are thus approximately stacked along the *a*-axis (Figure 2c).

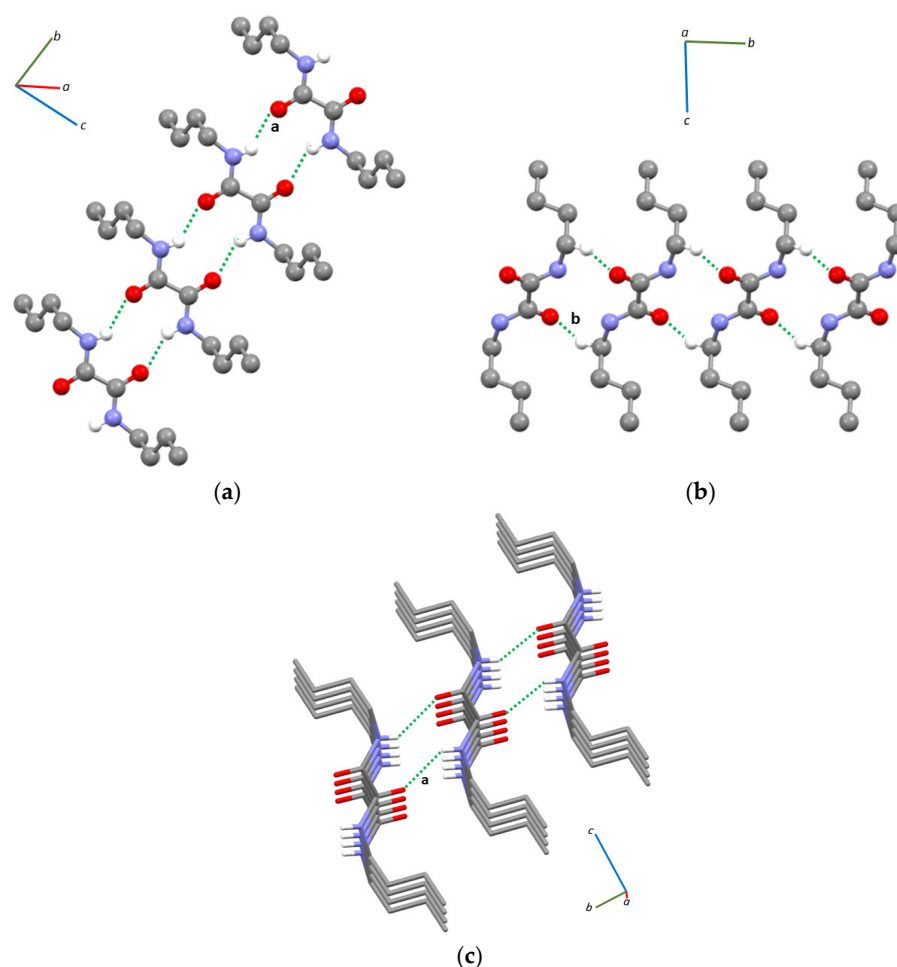


Figure 2. Intermolecular N–H...O hydrogen bonding (a) and C–H...O (b) interactions found in the crystal structure and partial view of the crystal packing of compound 1 (c); only hydrogen atoms involved in intermolecular interactions are shown for clarity. Labeling according to Table 1.

Table 1. Intermolecular interactions of compound 1.

Interaction		d_{D-H} (Å)	$d_{H...A}$ (Å)	$d_{D...A}$ (Å)	$\alpha_{D-H...A}$ (°)
a	N1 ⁱⁱ – H1 ⁱⁱ ...O1	0.86(2)	2.12(2)	2.8727(9)	146.9(16)
b	C4 ⁱⁱⁱ – H4 ⁱⁱⁱ ...O1	0.99	2.61	3.499(1)	149.0

Symmetry operations: ⁱⁱ = $x, -1 + y, z$; ⁱⁱⁱ = $1 + x, -1 + y, z$.

3. Materials and Methods

3.1. General Methods

Solvents and reagents were purchased from TCI (Chennai, India), FluoroChem (Haddington, UK), and Merck (Rahway, NJ, USA) and were used without further purification. Deuterated solvents were purchased from Eurisotop (Saint-Aubin-des-Bois, France) and stored over molecular sieves prior to use. FT-IR measurements were recorded at room temperature on a Thermo-Nicolet 5700 spectrometer (Thermo Fisher Scientific, Waltham, MA, USA) using KBr pellets with a KBr beam splitter and KBr windows ($4000\text{--}400\text{ cm}^{-1}$, resolution 4 cm^{-1}). ^1H and ^{13}C NMR spectra were carried out in CDCl_3 at room temperature using a Bruker Avance III HD 600 spectrometer (Bruker, Billerica, MA, USA). Chemical shifts are reported in ppm (δ) and were calibrated to the solvent residue. Elemental analysis was performed with a CHNS/O PE 2400 series II elemental analyzer ($T = 925\text{ }^\circ\text{C}$).

Uncorrected melting points were determined in capillaries on an FALC mod. C melting point apparatus.

3.2. X-ray Diffraction Analysis

X-ray diffraction data for compound **1** were collected at 120(2) K on a Rigaku FRE+ diffractometer (Rigaku, Tokyo, Japan), equipped with VHF Varimax confocal mirrors, an AFC12 goniometer, and a Saturn 724+ detector. The structure was solved with the ShelXT [34] solution program using dual methods and the model was refined with ShelXL 2018/3 [35] using full-matrix least-squares minimization of F^2 . Olex2 1.5 [36] was used as the graphical interface. All hydrogen atoms were included in the model at geometrically calculated positions and refined using a riding model, except for those of the N–H groups, which were refined freely.

3.3. Synthesis of *N,N'*-Dibutyloxamide (**1**)

Compound **1** was synthesized by a modification of a procedure described in the literature [24]: diethyloxalate (1.24 g; 8.50 mmol) in 5 mL of ethanol and *n*-butylamine (1.24 g; 17.0 mmol) in 5 mL of the same solvent were refluxed overnight. The mixture was cooled at room temperature and the white solid obtained was isolated by filtration on a Gooch funnel, washed with *n*-hexane, and air-dried. Colorless block-shaped crystals suitable for SC-XRD analysis were grown via the slow evaporation of an acetonitrile solution of the product (2.1 g; 10 mmol; yield = 63 %) M. p. = 152.8–153.5 °C (Lit.: 153–154 °C [24]). Elemental analysis calculated (%) for $C_{10}H_{20}N_2O_2$: C 59.97, H 10.07, N 13.99. Found: C 59.61, H 10.38, N 13.52. FT-IR (KBr, 4000–400 cm^{-1}): 3298 vs, 3062 w, 2955 s, 2930 m, 2873 m, 2862 m, 1650 vs, 1532 s, 1466 m, 1438 m, 1369 m, 1307 m, 1244 m, 1218 s, 1147 m, 1115 w, 977 w, 940 w, 759 vs, 557 s, 481 w, 465 w cm^{-1} . 1H NMR (600 MHz, $CDCl_3$) δ : 7.46 (s, br, 2H, NH), 3.31 (q, 4H, $CH_2CH_2CH_2CH_3$), 1.54 (quin, 4H, $CH_2CH_2CH_2CH_3$), 1.37 (sex, 4H, $CH_2CH_2CH_2CH_3$), 0.93 (t, 6H, $CH_2CH_2CH_2CH_3$) ppm. $^{13}C\{^1H\}$ NMR (151 MHz, $CDCl_3$) δ : 160.0, 39.5, 31.4, 20.1, 13.8 ppm.

4. Conclusions

The structural characterization of *N,N'*-dibutyloxamide (**1**), employed in recent years as a bridging ligand in the field of coordination chemistry, is reported in this paper. Compound **1** was synthesized by reacting diethyloxalate with *n*-butylamine and was fully characterized. Crystals suitable for SC-XRD were obtained by the slow evaporation of an acetonitrile solution of the compound, and the crystal structure shows two antiperiplanar amide groups and the *n*-butyl substituents protruding on opposite sides of the oxalamide plane. The crystal packing is governed by N–H \cdots O hydrogen bonding interactions leading to the formation of ribbons, which are held together by C–H \cdots O interactions.

Supplementary Materials: Figure S1: FT-IR spectrum; Figure S2: 1H -NMR spectrum; Figure S3: $^{13}C\{^1H\}$ -NMR spectrum; Figure S4: Portion of the crystal packing. Table S1: Crystal data and refinement parameters; Table S2: Bond lengths; Table S3: Bond angles; Table S4: Torsion angles.

Author Contributions: Conceptualization: A.P.; methodology: A.P., M.A. and M.C.A.; investigation: A.P., E.D. and E.P.; data curation: A.P., E.D., E.P. and S.J.C.; writing—original draft preparation: A.P.; writing—review and editing: A.P., E.D., E.P., M.A., M.C.A., V.L. and S.J.C. All authors have read and agreed to the published version of the manuscript.

Funding: The authors acknowledge Fondazione di Sardegna (FdS Progetti Biennali di Ateneo, annualità 2018) for financial support.

Data Availability Statement: Crystallographic data were deposited at CSD-CCDC (CIF deposition number 2266234).

Acknowledgments: CeSAR (Centro Servizi di Ateneo per la Ricerca) of the University of Cagliari is kindly acknowledged for NMR facilities.

Conflicts of Interest: The authors declare no conflict of interest.

References

1. Qiao, T.; Xiong, Y.; Feng, Y.; Guo, W.; Zhou, Y.; Zhao, J.; Jiang, T.; Shi, C.; Han, Y. Inhibition of LDH-A by Oxamate Enhances the Efficacy of Anti-PD-1 Treatment in an NSCLC Humanized Mouse Model. *Front. Oncol.* **2021**, *11*, 1033. [[CrossRef](#)] [[PubMed](#)]
2. Miskimins, W.K.; Ahn, H.J.; Kim, J.Y.; Ryu, S.; Jung, Y.-S. Synergistic Anti-Cancer Effect of Phenformin and Oxamate. *PLoS ONE* **2014**, *9*, 85576. [[CrossRef](#)] [[PubMed](#)]
3. Ogbu, I.M.; Kurtay, G.; Robert, F.; Landais, Y. Oxamic Acids: Useful Precursors of Carbamoyl Radicals. *Chem. Commun.* **2022**, *58*, 7593–7607. [[CrossRef](#)] [[PubMed](#)]
4. Ogbu, I.M.; Lusseau, J.; Kurtay, G.; Robert, F.; Landais, Y. Urethanes Synthesis from Oxamic Acids under Electrochemical Conditions. *Chem. Commun.* **2020**, *56*, 12226–12229. [[CrossRef](#)] [[PubMed](#)]
5. Maiore, L.; Aragoni, M.C.; Carcangiu, G.; Cocco, O.; Isaia, F.; Lippolis, V.; Meloni, P.; Murru, A.; Slawin, A.M.Z.; Tuveri, E.; et al. Oxamate Salts as Novel Agents for the Restoration of Marble and Limestone Substrates: Case Study of Ammonium N-Phenyloxamate. *New J. Chem.* **2016**, *40*, 2768–2774. [[CrossRef](#)]
6. Pintus, A.; Aragoni, M.C.; Carcangiu, G.; Giacometti, L.; Isaia, F.; Lippolis, V.; Maiore, L.; Meloni, P.; Arca, M. Density Functional Theory Modelling of Protective Agents for Carbonate Stones: A Case Study of Oxalate and Oxamate Inorganic Salts. *New J. Chem.* **2018**, *42*, 11593–11600. [[CrossRef](#)]
7. Maiore, L.; Aragoni, M.C.; Carcangiu, G.; Cocco, O.; Isaia, F.; Lippolis, V.; Meloni, P.; Murru, A.; Tuveri, E.; Arca, M. Synthesis, Characterization and DFT-Modeling of Novel Agents for the Protection and Restoration of Historical Calcareous Stone Substrates. *J. Colloid Interface Sci.* **2015**, *448*, 320–330. [[CrossRef](#)]
8. Aragoni, M.C.; Giacometti, L.; Arca, M.; Carcangiu, G.; Columbu, S.; Gimeno, D.; Isaia, F.; Lippolis, V.; Meloni, P.; Ezquerra, A.N.; et al. Ammonium Monoethyloxalate (AmEtOx): A New Agent for the Conservation of Carbonate Stone Substrates. *New J. Chem.* **2021**, *45*, 5327–5339. [[CrossRef](#)]
9. Curreli, F.; Kwon, Y.D.; Zhang, H.; Scacalossi, D.; Belov, D.S.; Tikhonov, A.A.; Andreev, I.A.; Altieri, A.; Kurkin, A.V.; Kwong, P.D.; et al. Structure-Based Design of a Small Molecule CD4-Antagonist with Broad Spectrum Anti-HIV-1 Activity. *J. Med. Chem.* **2015**, *58*, 6909–6927. [[CrossRef](#)]
10. Lip, G.Y.H.; Agnelli, G. Edoxaban: A Focused Review of Its Clinical Pharmacology. *Eur. Heart J.* **2014**, *35*, 1844–1855. [[CrossRef](#)]
11. Dong, K.; Elangovan, S.; Sang, R.; Spannenberg, A.; Jackstell, R.; Junge, K.; Li, Y.; Beller, M. Selective Catalytic Two-Step Process for Ethylene Glycol from Carbon Monoxide. *Nat. Commun.* **2016**, *7*, 12075. [[CrossRef](#)]
12. Zou, Y.Q.; Zhou, Q.Q.; Diskin-Posner, Y.; Ben-David, Y.; Milstein, D. Synthesis of Oxalamides by Acceptorless Dehydrogenative Coupling of Ethylene Glycol and Amines and the Reverse Hydrogenation Catalyzed by Ruthenium. *Chem. Sci.* **2020**, *11*, 7188–7193. [[CrossRef](#)]
13. Chen, Z.; Jiang, Y.; Zhang, L.; Guo, Y.; Ma, D. Oxalic Diamides and Tert-Butoxide: Two Types of Ligands Enabling Practical Access to Alkyl Aryl Ethers via Cu-Catalyzed Coupling Reaction. *J. Am. Chem. Soc.* **2019**, *141*, 3541–3549. [[CrossRef](#)]
14. Braun, M.; Frank, W.; Reiss, G.J.; Ganter, C. An N-Heterocyclic Carbene Ligand with an Oxalamide Backbone. *Organometallics* **2010**, *29*, 4418–4420. [[CrossRef](#)]
15. Nagarajprakash, R.; Govindarajan, R.; Manimaran, B. One-Pot Synthesis of Oxamidato-Bridged Hexarhenium Trigonal Prisms Adorned with Ester Functionality. *Dalt. Trans.* **2015**, *44*, 11732–11740. [[CrossRef](#)]
16. Nagarajprakash, R.; Divya, D.; Ramakrishna, B.; Manimaran, B. Synthesis and Spectroscopic and Structural Characterization of Oxamidato-Bridged Rhenium(I) Supramolecular Rectangles with Ester Functionalization. *Organometallics* **2014**, *33*, 1367–1373. [[CrossRef](#)]
17. Ramakrishna, B.; Divya, D.; Monisha, P.V.; Manimaran, B. Self-Assembly of Oxamidato-Chelated ReI- and MnI-Based Flexible Dinuclear Horse-Stirrup-Like Metallacycles. *Eur. J. Inorg. Chem.* **2015**, *2015*, 5839–5846. [[CrossRef](#)]
18. Ramakrishna, B.; Nagarajprakash, R.; Manimaran, B. One-Step Synthesis of Oxamidato Bridged Fac-Ru(CO)₃ Core Based Dinuclear Compounds: Spectroscopic and Structural Characterisation. *J. Organomet. Chem.* **2015**, *791*, 322–327. [[CrossRef](#)]
19. Ramakrishna, B.; Divya, D.; Kumar, U.; Mobin, S.M.; Manimaran, B. Self-Assembly of Mn(I)-Based Oxamidato-Bridged Dinuclear Molecular Tweezers and Tetranuclear Molecular Rectangles. *J. Organomet. Chem.* **2022**, *972*, 122371. [[CrossRef](#)]
20. Santana, M.D.; García, G.; Julve, M.; Lloret, F.; Pérez, J.; Liu, M.; Sanz, F.; Cano, J.; López, G. Oxamidate-Bridged Dinuclear Five-Coordinate Nickel(II) Complexes: A Magneto–Structural Study. *Inorg. Chem.* **2004**, *43*, 2132–2140. [[CrossRef](#)]
21. Casellato, U.; Guerriero, P.; Tamburini, S.; Vigato, P.A. Metal Complexes with Disubstituted Oxamidic Ligands. *Inorg. Chim. Acta* **1997**, *260*, 1–9. [[CrossRef](#)]
22. Mancuso, R.; Raut, D.S.; Della Ca, N.; Fini, F.; Carfagna, C.; Gabriele, B. Catalytic Oxidative Carbonylation of Amino Moieties to Ureas, Oxamides, 2-Oxazolidinones, and Benzoxazolones. *ChemSusChem* **2015**, *8*, 2204–2211. [[CrossRef](#)] [[PubMed](#)]
23. Meyer, T.; Rabeah, J.; Brückner, A.; Wu, X.F. Visible-Light-Induced Palladium-Catalyzed Dehydrogenative Carbonylation of Amines to Oxalamides. *Chem. Eur. J.* **2021**, *27*, 5642–5647. [[CrossRef](#)] [[PubMed](#)]
24. Rice, L.M.; Grogan, C.H.; Emmet, R. N,N'-Dialkyloxamides. *J. Am. Chem. Soc.* **1953**, *75*, 242. [[CrossRef](#)]
25. Desseyn, H.O.; Perlepes, S.P.; Clou, K.; Blaton, N.; Van Der Veken, B.J.; Dommissie, R.; Hansen, P.E. Theoretical, Structural, Vibrational, NMR, and Thermal Evidence of the Inter- versus Intramolecular Hydrogen Bonding in Oxamides and Thiooxamides. *J. Phys. Chem. A* **2004**, *108*, 5175–5182. [[CrossRef](#)]
26. CSD. *ConQuest Software*, Version 2022.1.0; The Cambridge Crystallographic Data Centre: Cambridge, UK, 2022.

27. Etter, M.C. Encoding and Decoding Hydrogen-Bond Patterns of Organic Compounds. *Acc. Chem. Res.* **1990**, *23*, 120–126. [[CrossRef](#)]
28. Bernstein, J.; Davis, R.E.; Shimoni, L.; Chang, N. Patterns in Hydrogen Bonding: Functionality and Graph Set Analysis in Crystals. *Angew. Chem. Int. Ed.* **1995**, *34*, 1555–1573. [[CrossRef](#)]
29. Nguyen, T.L.; Scott, A.; Dinkelmeyer, B.; Fowler, F.W.; Lauher, J.W. Design of Molecular Solids: Utility of the Hydroxyl Functionality as a Predictable Design Element. *New J. Chem.* **1998**, *22*, 129–135. [[CrossRef](#)]
30. Coe, S.; Kane, J.J.; Nguyen, T.L.; Toledo, L.M.; Wininger, E.; Fowler, F.W.; Lauher, J.W. Molecular Symmetry and the Design of Molecular Solids: The Oxalamide Functionality as a Persistent Hydrogen Bonding Unit. *J. Am. Chem. Soc.* **1997**, *119*, 86–93. [[CrossRef](#)]
31. Wen, Y.H.; Li, X.M.; Wang, L.; Zhang, S.S. N,N'-Diphenyloxalamide. *Acta Crystallogr. Sect. E Struct. Rep. Online* **2006**, *62*, o2185–o2186. [[CrossRef](#)]
32. Wen, Y.H.; Xu, L.L.; Li, X.M.; Zhang, S.S. N,N'-Bis(2-Methylphenyl)Oxamide. *Acta Crystallogr. Sect. E Struct. Rep. Online* **2006**, *62*, o3276–o3277. [[CrossRef](#)]
33. Wen, Y.H.; Zhang, K.; Li, X.M.; Bi, S.; Zhang, S.S. N,N'-Bis(3-Methoxyphenyl)Oxamide. *Acta Crystallogr. Sect. E Struct. Rep. Online* **2006**, *62*, o3443–o3444. [[CrossRef](#)]
34. Sheldrick, G.M. SHELXT—Integrated Space-Group and Crystal-Structure Determination. *Acta Crystallogr. Sect. A Found. Adv.* **2015**, *71*, 3–8. [[CrossRef](#)]
35. Sheldrick, G.M. Crystal Structure Refinement with SHELXL. *Acta Crystallogr. Sect. C Cryst. Struct. Commun.* **2015**, *71*, 3–8. [[CrossRef](#)]
36. Dolomanov, O.V.; Bourhis, L.J.; Gildea, R.J.; Howard, J.A.K.; Puschmann, H. OLEX2: A Complete Structure Solution, Refinement and Analysis Program. *J. Appl. Crystallogr.* **2009**, *42*, 339–341. [[CrossRef](#)]

Disclaimer/Publisher's Note: The statements, opinions and data contained in all publications are solely those of the individual author(s) and contributor(s) and not of MDPI and/or the editor(s). MDPI and/or the editor(s) disclaim responsibility for any injury to people or property resulting from any ideas, methods, instructions or products referred to in the content.